Fragmentation of fullerenes

Ryan T. Chancey,[1] Lene Oddershede,[2] Frank E. Harris,[1,3] and John R. Sabin[1,4]
[1]*Quantum Theory Project, P.O. Box 118435, University of Florida, Gainesville, Florida 32611*
[2]*The Niels Bohr Institute, Blegdamsvej 17, DK-2100 Copenhagen Ø, Denmark*
[3]*Department of Physics, University of Utah, Salt Lake City, Utah 84112*
[4]*Chemistry Department, University of Southern Denmark, 5230 Odense M, Denmark*
(Received 17 October 2002; published 22 April 2003)

We have performed classical molecular-dynamics simulations of the fragmentation collisions of neutral fullerenes (C_{24}, C_{60}, C_{100}, and C_{240}) with a hard wall. The interactions between the carbon atoms are modeled by a Tersoff potential and the position of each carbon atom at each time step is calculated using a sixth-order predictor-corrector method. The statistical distribution of the fragments depends on impact energy. At low energies, the fragment distribution appears symmetric, with both the large and small fragment distributions well fitted by an exponential function of the same exponent, the value of which decreases with impact energy. At intermediate energies, the distribution of the smallest fragments can be fitted equally well by a power law or an exponential function. At high impact energies, the entire fragmentation pattern is well described by a single exponential function, the exponent increasing with energy. The observed tendencies in fragment distributions as well as the obtained exponents are in agreement with experimental observations. The fragmentation behavior of the four investigated fullerenes is very similar, and it is noted that C_{60} appears to be the most stable.

DOI: 10.1103/PhysRevA.67.043203 PACS number(s): 36.40.Qv, 81.05.Tp, 82.20.Wt, 34.90.+q

I. INTRODUCTION

The beautiful symmetric structures of the fullerenes have received a large amount of recent attention [1], and have led people to suggest fullerenes for practical applications in the rapidly emerging field of molecular electronics [2]. The resistance of a single C_{60} has already been successfully measured [3], and a single fullerene has been proven to work as a transistor when placed within a gold nanojunction [4]. Related structures (carbon nanotubes) have also been shown to possess very promising characteristics for use in molecular electronics applications (e.g., as wires between gold contacts [5]). The stability of these unusual systems is crucial to their use in molecular electronic devices, and it is likely that the information we provide on the stability of fullerenes may also have implications for the stability of carbon nanotubes.

Surface-impact fragmentation patterns from objects ranging in size from meteorites [6] to gypsum balls [7] to atomic clusters consisting of thousands of atoms [8] are known to follow a power-law distribution, at least in the experimentally available impact energy regimes. On the other hand, an exponential fragment mass distribution has been observed for collisions of C_{60} ions with light target gases [9], suggesting a different fracture mechanism on the mesoscopic scale than on the larger scales. Moreover, experimental studies have reported a wide variety of fragment distributions for C_{60} [9–18]. On a smaller scale, the fragmentation of nuclei is well understood, the fragment mass distribution being well described by a statistical multifragmentation model [19] which predicts a qualitative dependence of fragment distribution on impact energy.

The present work complements the experimental studies by simulating the surface-impact fragmentation of C_{60} and the fullerenes C_{24}, C_{100}, and C_{240}. In our simulations, we have the advantage of being able to cover the entire range of energies from those producing no fragmentation to those which are large enough to yield total atomization of the fullerene. The simulated fragment distributions of the fullerenes have a qualitative as well as a quantitative dependence on the impact energy, thus helping to explain the differences among the experimental results.

Figure 1 shows snapshots from a simulated surface-impact fragmentation collision for a C_{60} fullerene, and from a collision at a lower energy for which no fragmentation takes place. Even though the lower energy is far larger than individual bond energies, we see (e.g., from the lower panel of Fig. 1) that the inelasticity is manifested by a conversion into vibrational energy without destruction of the cage structure.

II. SIMULATION METHOD

The fullerenes were modeled as collections of point atoms subject to the well-known classical interaction potential in-

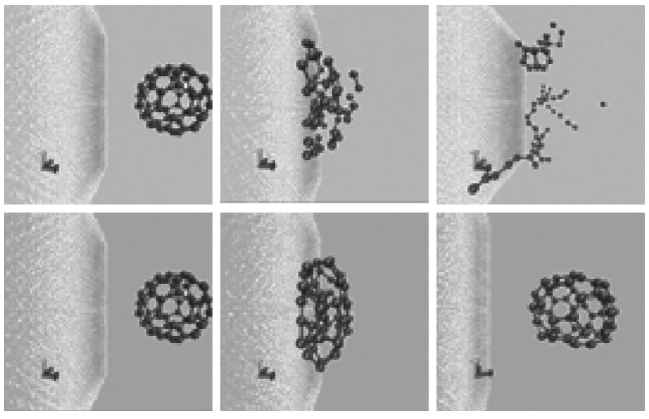

FIG. 1. Simulated surface-impact collision of a C_{60} fullerene at incident energies 300 eV (top) and 100 eV (bottom). From left to right: before, during, and after impact.

troduced by Tersoff [20]. The Tersoff potential is an empirical form that contains both two-body and angle-dependent three-body contributions and has parameters that were chosen to optimize the description of various solid phases of carbon, silicon, germanium, and their alloys. An initial static atomic configuration of each fullerene was obtained by starting from an experimentally reported structure [21] and relaxing to the equilibrium position consistent with the Tersoff potential. The appropriacy of the Tersoff potential was supported by the fact that in all cases the relaxation caused only minor position changes and removed small amounts of roundoff asymmetry from the experimental configuration.

The wall was modeled by a structureless potential of the form

$$V = V_0[1 - \tanh(\gamma z)], \tag{1}$$

where z is a cartesian coordinate normal to the wall. The parameters used were $V_0 = 100$ hartree and $\gamma = 1.0$ bohr^{-1}. This value of V_0 is high enough that, at all impact energies used, all atoms bounce back from the wall. The value of γ was chosen to make the wall comparable in steepness to a diamond surface. These parameter values make the potential negligible when all atoms are more than about 10 Å from the wall, but do not make the wall so steep that simulation becomes difficult. Earlier studies [22] indicate that the qualitative results are not sensitive to the details of the wall description or to its lack of atomic structure.

The simulations were initiated with the fullerene positioned outside the range of the wall potential, in its static equilibrium geometry, and with all atoms assigned a uniform velocity normal to the wall and consistent with the desired impact energy. Each simulation was started with a different random orientation of the fullerene, and this orientation distribution led to a distribution of fragmentation outcomes. Our earlier work [22] also showed that an assumption of nonzero initial temperature would have had little effect on the simulation statistics.

The dynamics was simulated by a stepwise integration of the classical equations of motion, using 0.1 fs time steps and a sixth-order Gear predictor-corrector formula [23]. This process was carried out using a computer program written by one of the authors. Most simulations were run for 2 ps (20 000 steps), and fragmentation was determined from the atomic positions at the end of the simulation. Based on the fact that the Tersoff potential has a finite-distance cutoff, we have chosen to define a fragment as a group of atoms each of which has a nonzero interaction with some other member of the group. A few runs were extended to 4 ps to see whether or not fragmentation at earlier times was essentially complete. These, and earlier studies that also examined the energies of individual fragments, were consistent with the conclusion that little fragmentation, and essentially no recombination, would occur after the first picosecond.

For C_{60}, fragmentation statistics at each impact energy were accumulated by making batches of 1000 trajectories (with the orientations in each batch random with respect to those in the other batches), and these batches were then combined to provide overall statistics on 8000-trajectory samples. These data enabled us to verify that the statistics did not vary with sample size for batches of 1000 trajectories or more. Sets of 1000 trajectories were then run for each of the other fullerenes.

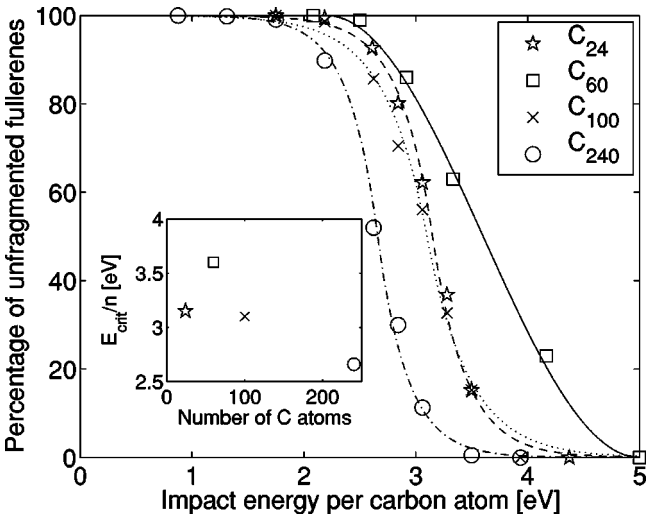

FIG. 2. Percentage of fullerenes that remain unfragmented as a function of impact energy per carbon atom. The inset shows E_{crit}/n for each of the investigated fullerenes.

The use of a structureless wall and efficient computer programming enabled us to produce a large number of simulations with a modest consumption of computer resources. As an example, a 20 000 step trajectory for a C_{60} fullerene required approximately 67 s on a Sun Sparc Ultra 5 (a serial workstation).

III. STABILITY OF FULLERENES

Figure 2 shows the percentage (based on 1000 trajectories) of each of the fullerenes that remains unfragmented as a function of the impact energy per carbon atom. One way to characterize the stability with respect to surface impact is to determine the energy at which 50% of the fullerenes have fragmented; we denote this energy E_{crit}. From Fig. 2, E_{crit}/n (where n is the number of carbon atoms in the fullerene) was found for each type of fullerene and in the inset, this quantity is plotted against n. As is seen there, the C_{60} fullerene appears more stable with respect to fragmentation than the other investigated fullerenes.

We find the values of E_{crit}/n to be in the interval 2.7–3.6 eV per carbon atom. As the average bond strengths of fullerenes are of the order of 4–5 eV, the data indicate that even after impact, the bulk of the incident kinetic energy remains widely distributed among the atoms of the molecule. This behavior at energies insufficient to fragment the molecule was noted by Mowrey *et al.* [24], who referred to it as ''resilience.''

IV. FRAGMENT DISTRIBUTION

The fragment distributions from the collisions of the fullerenes against a hard wall are shown in Figs. 3, 4, 5, and 6 for C_{24}, C_{60}, C_{100}, and C_{240}, respectively. The data shown

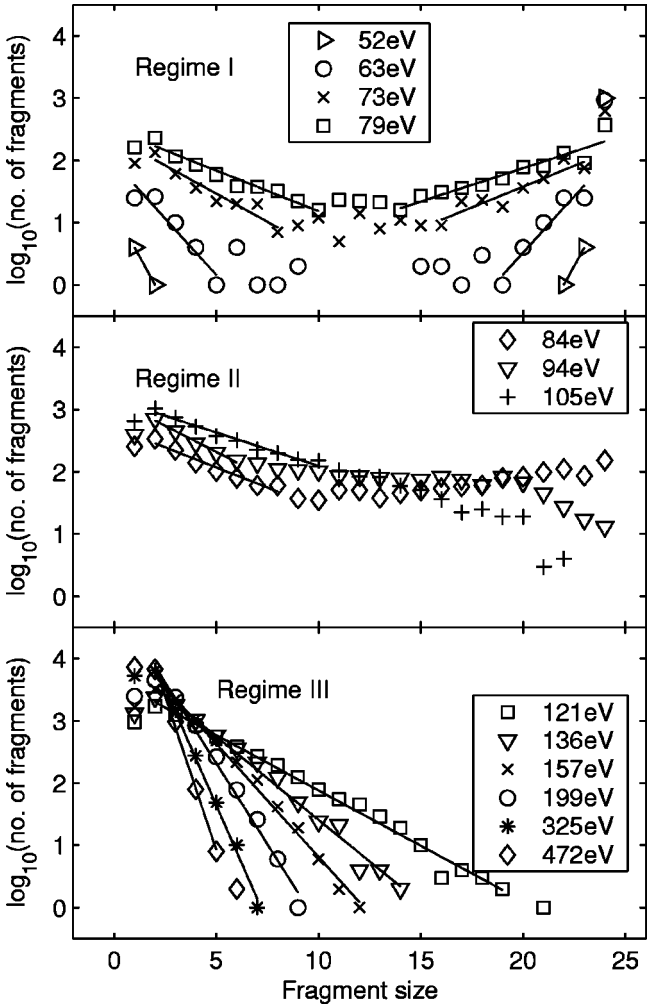

FIG. 3. Fragment distribution from 1000 events of C_{24} impact on a hard wall at various impact energies ranging from 52 to 472 eV.

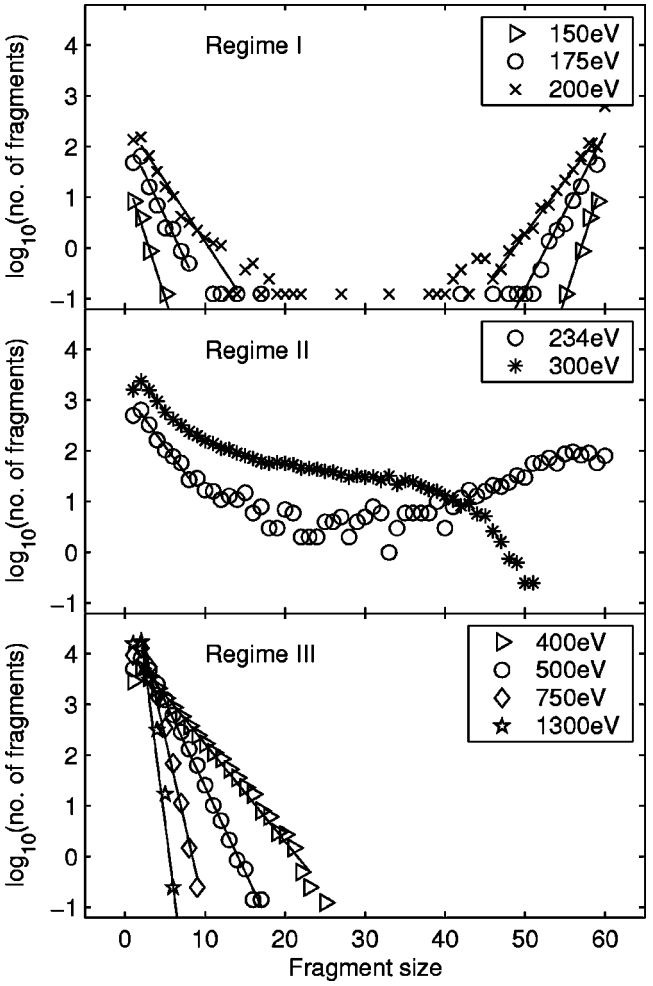

FIG. 4. Fragment distribution per 1000 events of C_{60} impact on a hard wall at various impact energies ranging from 150 to 1300 eV.

span the range from the lowest energy at which any fragmentation occurs to the highest energy that has not led to full atomization. The points on the plots indicate the total numbers of fragments of each size in a 1000-trajectory sample. For C_{60}, the raw data consisted of eight times 1000 trajectories and the numbers shown in Fig. 4 are the average numbers of fragments from a 1000-trajectory sample; for the other fullerenes, 1000-trajectory data was used directly. If there are no fragments of a given size, its mark is omitted. To avoid overly dense plots, only about half of the available data sets are shown. Also, for the sake of clarity, in Fig. 5, only alternate fragment sizes were marked; in Fig. 6, the marking was reduced to every fourth fragment size. All the data obtained in this study are available from the authors.

The full lines in Figs. 3–6 are fits of the data to the exponential form

$$N(s) = C_1 \exp(-\alpha s), \tag{2a}$$

or, in the right-hand side of the top panels,

$$N(s) = C_2 \exp(-\beta[n-s]), \tag{2b}$$

where $N(s)$ is the number of fragments of size s; n is the number of carbon atoms in the fullerene; and α, β, C_1, and C_2 are constants. The exponential form in Eq. (2a) is chosen as a fit to data partly because similar functional forms have been found to fit experimental data from the fracture of fullerenes quite well [9], and partly because as demonstrated in Ref. [19] the exponential functional form describes the fragments distribution following a breakup of atomic nuclei in certain energy regimes, and a similar description, though not carried out yet, might be valid for the mesoscopic regime of the fullerenes too. Equation (2b) is used as a fit to the distribution of large fragments in the low impact energy regime, but does not carry any physical information. It simply demonstrates the physical fact that the fullerene breaks into two parts, with neither undergoing further fragmentation, and hence the fragmentation distribution is symmetric in the small and large fragments (apart from the point originating from the unfragmented fullerenes) and both the small and large fragments are equally well fit by the exponential functions in Eqs. (2a) and (2b) with identical exponents $\alpha = \beta$.

As evident from Figs. 3–6, the appearance of the fragment distribution depends upon the impact energy. We have, therefore, divided the fragment distributions into three regimes and defined the different regimes as follows.

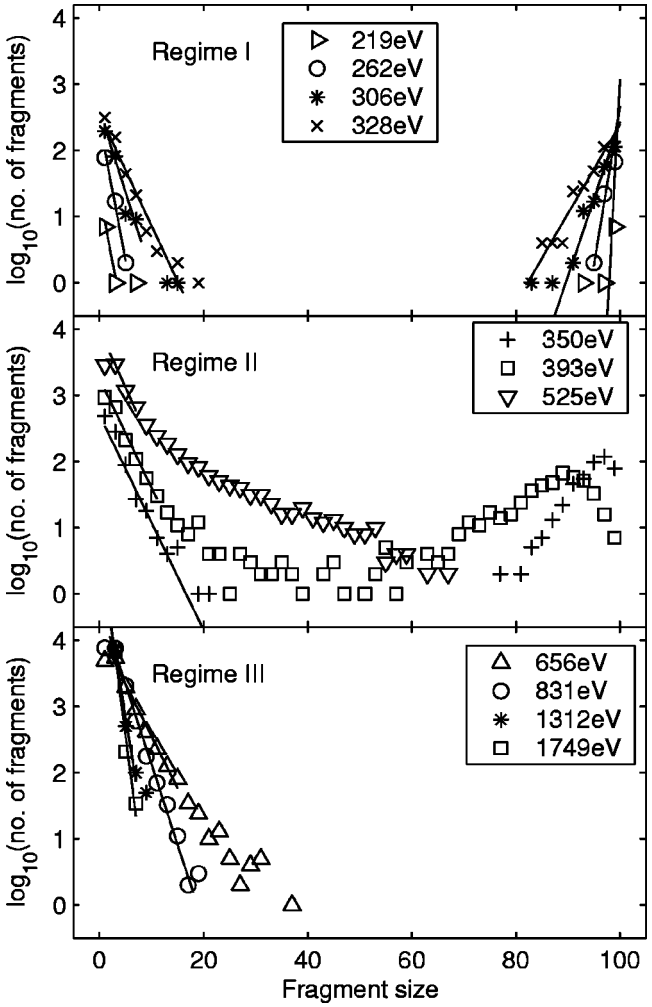

FIG. 5. Fragment distribution from 1000 events of C_{100} impact on a hard wall at various impact energies ranging from 219 to 1749 eV.

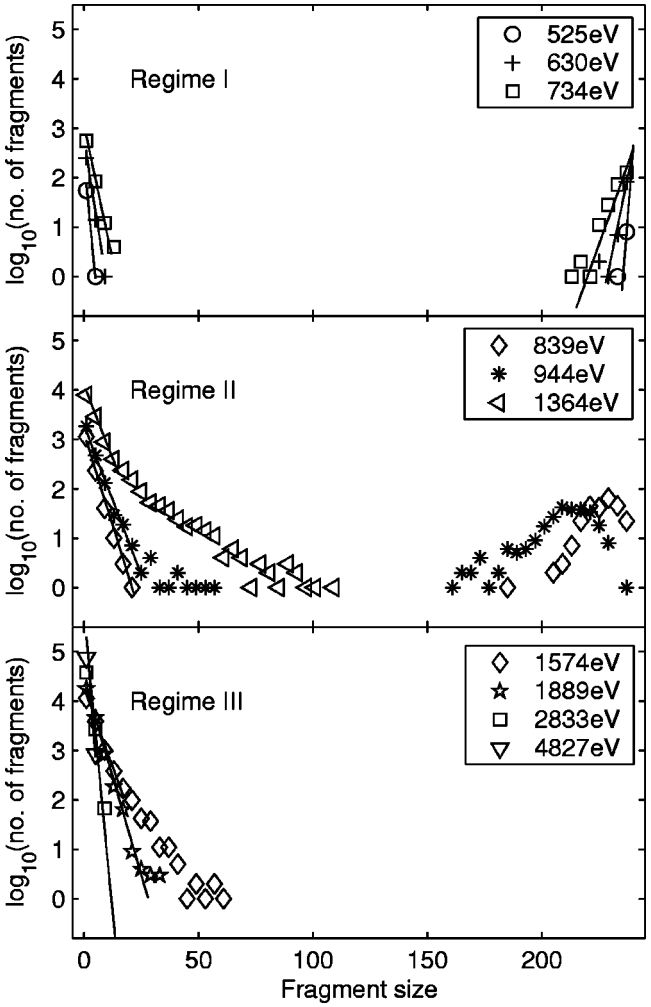

FIG. 6. Fragment distribution from 1000 events of C_{240} impact on a hard wall at various impact energies ranging from 525 to 4827 eV.

(a) Regime I. This regime comprises the low impact energies, where the distribution appears mirror symmetric between the large and small fragments. See the upper panels of Figs. 3–6. The data indicate a preference for the break off of small fragments. Also, we see that the numerical value of the exponent from Eqs. (2a) and (2b) decreases with increasing impact energy, consistent with the fact that greater energy leads to more extensive fragmentation.

(b) Regime II. As impact energies are increased, the fragment distribution ceases to be symmetric, and the fraction of large fragments decreases because multiple fragmentations of the fullerenes now occur. The distribution of large fragments is not well fit by an exponential function. However, the small-fragment distribution can still be fit (as shown) by an exponential function, the exponent being only weakly dependent on the impact energy. In fact, this part of the distribution could also be fit by a power law (fitting not shown). Regime II is shown in the middle panels of Figs. 3–6.

(c) Regime III. At high impact energies, the entire fragment distribution is fitted well by the exponential distribution of Eq. (2a), so α^{-1} denotes the average size of a fragment and C_1 is a normalization factor. In this regime, α increases with energy. Fragment distributions belonging to regime III are shown in the lower panels of Figs. 3–6.

Based on the above definitions, we have determined the energies at which the transitions between the regimes occur for the four investigated fullerenes. Since the definitions are not exact and the data are from discrete impact energies, the values of the transition energies are given as intervals. For each of the fullerenes C_{24}, C_{60}, C_{100}, and C_{240}, both the absolute values of the transition energy and the transition impact energy per carbon atom are given in Table I. For all investigated fullerenes, the transition between regimes I and II occurs at impact energies near 3.4 eV per carbon atom. The transition between regimes II and III is near 5.3 eV.

We look next at the parameters describing the fragment distributions, i.e., the quantities α occurring in Eq. (2a). The α values for the four investigated fullerenes are presented as a function of the impact energy per carbon atom in Fig. 7. This figure exhibits the tendencies identified in our earlier descriptions of the various fragmentation regimes. At low impact energies (regime I), all four fullerenes have similar α values, decreasing with impact energy, probably indicative of a similarity in the mechanisms whereby small moieties are

TABLE I. Intervals containing the transition impact energy between regimes I and II, and between regimes II and III for all investigated fullerenes.

Fullerene	I–II (eV)	I–II (eV/carbon)	II–III (eV)	II–III (eV/carbon)
C_{24}	79–84	3.3–3.5	105–121	4.4–5.0
C_{60}	200–234	3.3–3.9	300–400	5.0–6.7
C_{100}	328–350	3.3–3.5	525–656	5.3–6.6
C_{240}	734–839	3.1–3.5	1364–1574	5.7–6.6

detached from the incoming molecule. The full line in Fig. 7 is a linear fit to the exponents in this range. Letting E_r denote the impact energy per carbon atom, the line is described by the equation $\alpha = 1.2 - 0.34E_r$.

In regime II, the α values fall between 0.1 and 0.2. No simple generalization is available for this regime.

At large impact energies (regime III), the average fragment size (α^{-1}) decreases with increasing impact energy. The fullerenes also differ in the way α depends upon E_r: For a given E_r, the average size of the fragments from a C_{24} or C_{60} fullerene is smaller than that from a fragmented C_{100} or C_{240}. This could be because the larger fullerenes have more opportunities to stabilize fragments of intermediate size, whereas the smaller shatter more completely. The dotted and dashed lines are linear fits to the α values of, respectively, the C_{100} and the C_{24} fullerenes, corresponding to the equations $\alpha = -0.06 + 0.04E_r$ and $\alpha = 0.03 + 0.05E_r$. The purpose of the fits in this figure is to provide an easier comparison to experiments.

V. DISCUSSION

The qualitative variation found here for the fragment distribution with impact energy is similar to the distributions resulting from the breakup of atomic nuclei. In Ref. [19], the statistical multifragmentation model is put forward as a thermodynamic description on the breakup of nuclei, based on the assumption that the nuclei are in equilibrium both before and immediately after the impact. One result of this statistical multifragmentation model is that the fragment mass distribution varies with impact energy and is a result of the dominating disintegration mechanism in that particular energy regime. Regime I in this paper corresponds to the ''compound nucleus'' regime in Ref. [19], regime II corresponds to ''fission like processes'' and ''fragmentation onset,'' and regime III corresponds to the ''multifragmentation'' and ''nuclear gas'' regimes. At this point, a similar statistical ensemble description of the fullerene system based on the free energy and entropy of the system at various temperatures does not exist in the literature. However, the similarities between our results and those theoretically predicted for a nuclear system in Ref. [19] are striking, and it is very likely that a similar description, though not yet available, would be valid for the fullerenes too.

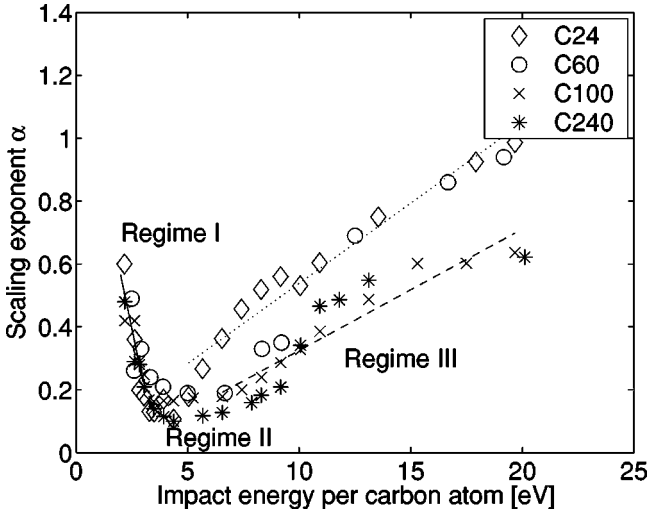

FIG. 7. Exponent α of Eqs. (2a) and (2b) as a function of impact energy per carbon atom.

Fragmentations of fullerenes have been examined experimentally both by collisions with atoms, ions, or small molecules [9–15], and by surface-impact studies [16–18]. These experiments involve beams of fullerene ions (cations and/or anions) aimed at gaseous targets or surfaces, with the collision products usually identified by mass spectrometry. Physically, our simulated results are closer to the experimental surface impact studies than to the target gas impact studies. However, for studies of fragment distributions on larger scales, it has been postulated that the distributions of, e.g., gypsum rods, plates, and balls are not very dependent upon the fragmentation method [7,25,26].

Hvelplund and co-workers [9,10] have suggested that the primary events in fullerene-atom collisions are successive ''knockouts'' of small fragments, followed by a delayed ''annealing'' process in which single carbon atoms are ejected from species containing odd numbers of carbon atoms as the cage structure is healed. The time scale of such processes far exceeds our simulation capabilities, and the studies we have made are not applicable to repeated collisions with gas molecules. Nevertheless, it is interesting to note that Hvelplund *et al.* report that fragment distributions from C_{60}-H_2 collisions at 50–200 keV can be described by equations similar to Eq. (2a) of this paper. They find α values in the range 0.18–0.23 and decreasing with increasing impact energy, as in regime I. However, for C_{60}-He collisions in the same energy range, these authors find α values in the range 0.14–0.17 and increasing with energy, as in regime II. Thus, despite the fact that we are looking at neutral fullerenes, while they studied ions, the results show a high degree of similarity. But because the breakup mechanism in their work differs from that in our simulations, the regime transitions will occur at different ranges of impact energy. In Ref. [10], the same group has noted a strong dependence of the fragmentation pattern on the choice of target atom number, with fragment distributions that correspond very well to those obtained in this paper. For example, Fig. 9 of Ref. [10] shows fragment distributions corresponding to our regime I, though the impact energies are substantially larger. We do not see a preference of even numbered carbon species as observed upon the fracture of C_{60}^+, e.g., in Refs. [9,17].

In Ref. [11], a bimodal fragment distribution is observed resulting from the fracture of C_{60} ions with rare-gas atoms at 200 eV. This result is consistent with our findings at 200 eV for C_{60}. It has also been reported [13] that collisions between Si^{q+} projectiles and a C_{60} target yield a distribution of small C_n fragment ions ($n=1-12$) which is approximated fairly well by a power law. This observation is also consistent with our findings for the smallest fragments in regime II, where we find that both exponential forms and power laws are valid approximations to the fragment distribution. Again, due to the different fracture mechanisms, the size of impact energies cannot be compared.

Turning now to the surface-impact experiments [16–18], which are more directly comparable with the present study, we note that all are consistent with our observation that impact energies far larger than the bond energies are required for fragment ejection. The earliest of the studies we examined, that of Busmann *et al.* [16], indicated little fragmentation for collisions of C_{60}^+ either with diamond or graphite surfaces below about 150 eV. Up to 500 eV, the energetic limit of their study, the larger fragments corresponded to the loss of one or more C_2 units, with most of the material in clusters of 50 or more atoms. The distribution of the small fragments was not reported.

Beck *et al.* [17] examined not only C_{60}^+, but also several larger fullerene cations (up to C_{164}^+) at impact energies between 150 and 1050 eV. They concluded that at energies near the fragmentation threshold, the data were consistent with a mechanism that involved the ejection of C_2 units, but that at higher impact energies, the fullerene ''shatters'' into a large number of smaller fragments. The fragment distribution, provided, e.g., in Fig. 2 of Ref. [17], is qualitatively in agreement with our findings and shows similar changes as a function of impact energy. A more quantitative comparison is precluded by the limited precision with which the plotted data can be read. Further discussion of the high-energy shattering process is provided in another contribution of Beck *et al.* [18] and again, they find that the fragment distribution switches from a U shape to an S shape and finally to a power law, in agreement with the transition from regime I to II to III which is described in this paper.

It has been speculated that collisions might fission a large fullerene into smaller cage molecules (e.g., $C_{240} \rightarrow 4C_{60}$, or at least to one C_{60} plus other fragments). Our data show no such preference for ''magic numbers'' among the fragments.

VI. CONCLUSIONS

We have presented a classical molecular-dynamics simulation study of the fragmentation of the C_{24}, C_{60}, C_{100}, and C_{240} fullerenes upon impact with a hard wall by using a Tersoff potential to model the C-C interactions. The resulting fragment distributions depend both qualitatively and quantitatively on the impact energy. Our results reproduce the observed fragment distributions in the limited energy ranges within which experiments have been carried out, and go beyond them such that our energy range is substantially larger and that we are not limited to fullerenes that are available for experimentation. We have divided the fragmentation distributions into three different regimes. Similar regimes have been theoretically predicted and experimentally observed in the fragmentation of atomic nuclei. Hence, the fracture process of a fullerene more resembles that of an atomic nucleus than that of a larger object, say a gypsum ball, which in literature typically is reported to produce a power-law distribution of fragments. However, a full thermodynamical description of fullerene fragmentation is still a challenge for the future. Also, our results show that the C_{60} fullerene is more stable towards fragmentation than the other investigated fullerenes.

ACKNOWLEDGMENTS

We would like to thank J. P. Bondorf and H. Flyvbjerg for fruitful suggestions and discussions. This work was supported by the National Science Foundation (R.T.C. and F.E.H., Grant No. DMR-9980015; J.R.S., Grant No. CHE-9974385), and by the U.S. Office of Naval Research (J.R.S., Grant No. N0014-96-1-0707).

[1] H. Handschuh, G. Ganteför, B. Kessler, P.S. Bechthold, and W. Eberhardt, Phys. Rev. Lett. **74**, 1095 (1995).
[2] C. Joachim, J.K. Gimzewski, and A. Aviram, Nature (London) **408**, 541 (2000).
[3] C. Joachim, J.K. Gimzewski, R.R. Schlittler, and C. Chavy, Phys. Rev. Lett. **74**, 2102 (1995).
[4] H. Park, J. Park, A.K.L. Kim, E.H. Anderson, A.P. Alivisatos, and P.L. McEuen, Nature (London) **407**, 57 (2000).
[5] M.S. Fuhrer, J. Nygard, L. Shih, M. Forero, Y.G. Yoon, M.S.C. Mazzoni, H.J. Choi, J. Ihm, S.G. Louie, A. Zettl, and P.L. McEuen, Science **288**, 494 (2000).
[6] L. Oddershede, A. Meibom, and J. Bohr, Europhys. Lett. **43**, 598 (1998).
[7] L. Oddershede, P. Dimon, and J. Bohr, Phys. Rev. Lett. **71**, 3107 (1993).
[8] A. Kuhle, L. Oddershede, and J. Bohr, Z. Phys. D: At., Mol. Clusters **40**, 523 (1997).
[9] P. Hvelplund, L.H. Andersen, H.K. Haugen, J. Lindhard, D.C. Lorents, R. Malhotra, and R. Ruoff, Phys. Rev. Lett. **69**, 1915 (1992).
[10] M.C. Larsen, P. Hvelplund, M.O. Larsson, and H. Shen, Eur. Phys. J. D **5**, 283 (1999).
[11] R. Ehlich, O. Knospe, and R. Schmidt, J. Phys. B **30**, 5429 (1997).
[12] T. Kunert and R. Schmidt, Phys. Rev. Lett. **86**, 5258 (2001).
[13] A. Itoh, H. Tsuchida, K. Miyabe, T. Majima, and Y. Nakai, Phys. Rev. A **64**, 032702 (2001).
[14] R. Vandenbosch, Phys. Rev. A **64**, 033201 (2001).
[15] L. Chen, S. Martin, R. Brédy, J. Bernard, and J. Désesquelles, Phys. Rev. A **64**, 031201 (2001).
[16] H.-G. Busmann, T. Lill, B. Reif, I.V. Hertel, and H.G. Maguire, J. Chem. Phys. **98**, 7574 (1993).
[17] R.D. Beck, J. Rockenberger, P. Weis, and M.M. Kappes, J.

Chem. Phys. **104**, 3638 (1996).
[18] R.D. Beck, C. Warth, K. May, and M.M. Kappes, Chem. Phys. Lett. **257**, 557 (1996).
[19] J.P. Bondorf, A.S. Botvina, A.S. Iljinov, I.N. Mishustin, and K. Sneppen, Phys. Rep. **257**, 133 (1995).
[20] J. Tersoff, Phys. Rev. B **39**, 5566 (1989).
[21] See, coordinates for C_{24} and C_{240}: URL http://www.ccl.net/cca/data/fullerenes/; for C_{60} and C_{100}: http://shachi.cochem2.tutkie. tut.ac.jp/Fuller/higher/higherE.html
[22] Q.-H. Tang, K. Runge, H.-P. Cheng, and F.E. Harris, J. Phys. Chem. A **106**, 893 (2002).
[23] C.W. Gear, *Numerical Initial Value Problems in Ordinary Differential Equations* (Prentice-Hall, Englewood Cliffs, 1971).
[24] R.C. Mowrey, D.W. Brenner, B.I. Dunlap, J.W. Mintmire, and C.T. White, J. Phys. Chem. **95**, 7138 (1991).
[25] T. Kadono, Jpn. J. Appl. Phys., Part 2 **36**, L1221 (1997).
[26] T. Kadono, Phys. Rev. Lett. **78**, 1444 (1997).